J Mater Sci: Mater Med (2008) 19:1317–1323
DOI 10.1007/s10856-007-3158-7

Mechanical properties of open-cell foam synthetic thoracic vertebrae

Amy E. Johnson · Tony S. Keller

Received: 19 April 2006 / Accepted: 21 August 2006 / Published online: 20 September 2007

Abstract This study presents comprehensive morphological and mechanical properties (static, dynamic) of open-cell rigid foams (Pacific Research Laboratories Inc. Vashon, WA) and a synthetic vertebral body derived from each of the foams. Synthetic vertebrae were comprised of a cylindrical open-cell foam core enclosed by a fiberglass resin cortex. The open-cell rigid foam was shown to have similar morphology and porosity as human vertebral cancellous bone, and exhibited a crush or fracture consolidation band typical of open-celled materials and cancellous bone. However, the foam material density was 40% lower than natural cancellous bone resulting in a lower compressive apparent strength and apparent modulus in comparison to human bone. During cyclic, mean compression fatigue tests, the synthetic vertebrae exhibited an initial apparent modulus, progressive modulus reduction, strain accumulation and S-N curve behaviour similar to human and animal vertebral cancellous bone. Synthetic open-cell foam vertebrae offer researchers an alternative to human vertebral bone for static and dynamic biomechanical experiments, including studies examining the effects of cement injection.

Presented, in part, at the XXth Congress of the International Society of Biomechanics and 29th Annual Meeting of the American Society of Biomechanics, Cleveland, OH, July 31-August 5, 2005

A. E. Johnson
Department of Mechanical Engineering, The University of Vermont, Burlington, VT, USA

T. S. Keller (✉)
Florida Orthopaedic Institute, 13020 Telecom Parkway N, Temple Terrace, FL 33637-0925, USA
e-mail: tkeller@floridaortho.com

Introduction

The design or structure of bone in human vertebrae and elsewhere in the body is very complex ranging from a very porous cellular solid (cancellous or trabecular bone) to a very dense solid (cortical or compact bone) [1]. Polyurethane rigid foams and fiberglass epoxy resins are currently used as substitutes for natural bone in biomechanical tests because they have similar mechanical properties, such as stiffness and strength to cadaveric bone [2, 3]. Synthetic materials intended for biomechanical tests reduce inter-specimen variation, are easy to handle, do not degrade and are generally low in cost in comparison to natural bone. Commercially available synthetic bone material substitutes have been developed for a variety of anatomic structures (primarily long bones), but there are currently no commercially available synthetic vertebrae bodies, which are comprised primarily of cancellous bone surrounded by a very thin cortical shell ($\sim$2 mm).

Both open-cell and closed-cell foam materials are commercially available for use as a synthetic substitute for trabecular bone, but each exhibit different responses to mechanical loads. Closed-cell foam exhibits similar static mechanical properties to human cancellous bone, however its fatigue behaviour exhibits different S-N curve characteristics and a lesser degree of modulus degradation and accumulation of permanent strain under cyclic loading [4]. The walls of closed-cell foams stretch whereas cell edges in open-cell structures bend, resulting in variable strain response to applied stress [5, 6]. Compressive fatigue failure mechanics also differ between open and closed-cell foams in the formation of the crush zone. The crush zone for open-cell foams initially involves the whole specimen uniformly, then progressively shortens until the crush band involves a localized band of single cells, which is more

characteristic of trabecular bone whereas under the same strain, closed-cell foam crush zone initiates in a localized band and expands to involve surrounding cells [5, 7].

A synthetic material that can be used in static and fatigue studies for vertebral cement augmentation has not yet been identified. Cement augmentation is a percutaneous method used to reinforce osteoporotic trabecular bone. An open-cell structure, which more closely resembles the porous network of trabecular bone, permits cement infiltration. The objectives of the current work were to (i) evaluate the morphological and mechanical properties of a rigid open-cell, polyurethane foam material, and (ii) develop a synthetic thoracic vertebrae that could be used for future cement augmentation studies. Apparent strength, stiffness, hysteresis and fatigue properties of the synthetic vertebrae are presented.

Methods

Morphology measurements and static compression tests were performed on specimens of open cell, polyurethane foam alone. Dynamic mechanical tests were then conducted on synthetic vertebrae comprised of the foam core surrounded by a fiberglass resin cortex.

Open-cell rigid foam morphology

Blocks of open cell rigid foam of apparent density, (ρ_{a1} = 0.12 g/cm^3 and ρ_{a2} = 0.09 g/cm^3) were obtained from Pacific Research Laboratories, Inc. (Vashon Island, WA). Nine millimeter diameter foam cubes of each density were digitized using a μCT scanner (36 micron voxels). Volume fraction (BV/TV), three-dimensional (3D) material anisotropy, and standard morphology were characterized using a proprietary program based on the parallel plate model method [8]. Standard 2D and 3D morphology parameters include, bone surface/bone volume ratio (BS/TV), trabecular number (Tb.N), trabecular thickness (Tb.Th) and trabecular spacing (Tb.Sp). Three mean intercept lengths (MIL 1,2,3) for anisotropy characterization and a trabecular connectivity index (TCI) were determined wherein a higher index indicates a higher degree of connectivity. Material density, $\rho_{material}$ of the foam was determined by dividing the apparent density of each foam by their respective volume fraction, $\rho_{material} = \rho_a$ /BV/TV.

Static compression tests

Ten samples of 0.12 g/cm^3 open cell foam were cut into cylindrical cores (12.8 mm diameter by 19.8 mm height) using a brass-coring tool. The cylindrical foam samples were initially subjected to non-destructive uniaxial compression tests under displacement control using a servo-hydraulic test machine. Specimens were preloaded to 0.5N, preconditioned for 5 cycles to 0.5% strain using a 1 Hz sinusoid, and ramp loaded at 0.16 mm/s to 1% strain. 1.5 mm thick fiberglass resin endplates were molded to the top and bottom surfaces of the foam samples (Fig. 1). This protocol was adopted from a fatigue study of bovine trabecular bone that used this test method to determine the appropriate stress range for subsequent fatigue tests [9].

The fiberglass resin endplate was representative of the cortical bone endplate present in vertebrae, and served to reinforce the damaged (cut), load-bearing surface of the foam cylinders. Foam cores with endplates were non-destructively tested as described previously, followed by a failure ramp at the same displacement rate of 0.16 mm/s. A subsequent group of ten 0.12 g/cm^3 foam samples without fiberglass endplates were tested to failure under the same protocol to obtain yield and ultimate mechanical properties.

Stress-strain data were used to obtain the apparent modulus (E_a), 0.2% offset yield stress (σ_y), 0.2% offset yield strain (ε_y), ultimate stress (σ_{ult}), and ultimate strain (ε_{ult}), hysteresis (H), and modulus of resilience (E_{res}). Hysteresis determined from the area enclosed by one cycle on a stress-strain plot divided by the total area underneath the loading half of the cycle. The modulus of resilience is the total area underneath a loading curve up to failure on a plot of stress versus strain. The apparent elastic modulus was also determined over a low strain range (<0.5%) and a high strain range (0.5–1.0%) for the non-destructive tests.

Synthetic thoracic vertebrae

After morphology and static properties of the open-cell foam were characterized, the foam was used to create synthetic vertebrae comprised of a simplified cylindrical

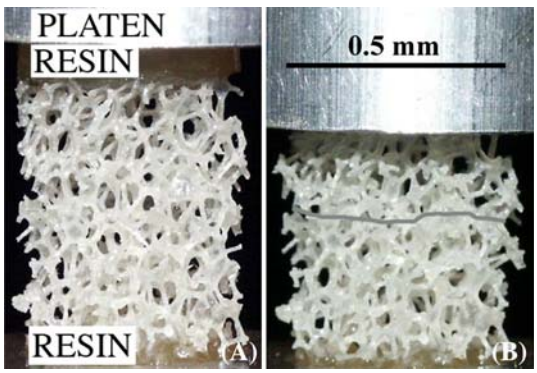

Fig. 1 (**A**) Foam sample with fiberglass endplates prior to compression; (**B**) Crush zone (highlighted) is visible at failure

geometry surrounded by a fiberglass resin cortex. Two different densities of open cell foam were cut into forty-four cylindrical cores similar in size to T6–T8 thoracic vertebral centrum (30 mm diameter by 19.8 mm height). The diameter for the cores was determined from averaged endplate anterior–posterior and lateral–medial lengths of 221 T6–T12 vertebrae [10, 11]. A thin layer (~2 mm) of fiberglass resin was applied to the surfaces of the cylindrical cores to simulate the cortical cortex. The fiberglass resin was thickened with a low-density filler to facilitate application of the cortex. The diameter and height of each synthetic thoracic specimen was measured with calipers and averaged over three measurements.

Dynamic compression tests

Synthetic thoracic vertebrae were cycled to failure using 10 different, mean compression stress ranges ($\Delta\sigma$ = peak stress–minimum stress, minimum stress = 0.26 MPa, approximate body weight supported by the thoracic spine in a 66 kg person). Peak stresses were varied to produce low cycle ($<10^4$ cycles) and high cycle ($>10^4$ cycles) fatigue failure. The resulting peak compressive stress range applied to the synthetic vertebrae was consistent with in vivo disc pressure measurements obtained during postural loading physiological conditions (0.5 MPa for relaxed standing to 2.3 MPa for lifting 20 kg) [12]. Load-displacement data was collected every 10th cycle at a sampling rate of 100 Hz in order to have 50 data points to describe each loading cycle.

The initial modulus (E_o) was determined over a 0.2% strain range and was used to calculate the effective strain ($\Delta\sigma/E_o$). Fatigue failure was defined at 30% modulus reduction or at the last cycle before rapid deformation [5, 13, 14]. The modulus was calculated from the slope of the loading portion of each hysteresis loop. Strain accumulation was characterized by two values, cyclic creep and damage strain. The latter is defined as the translation of the hysteresis loop along the strain axis and the change in strain within each hysteresis loop, respectively (Fig. 2). Scalar values representing cyclic creep and damage strain were computed from the area under each strain vs. cycle curve and normalized by the total strain curve area. Total strain was defined as the sum of cyclic creep and damage strain.

Compression fatigue behaviour of trabecular bone is characterized by non-linear modulus reduction, progressive shortening and an effective strain range between 0.003 and 0.009 [9]. Non-linear modulus reduction in cortical bone has been shown to be a function of life fraction, n/N_f in an empirical relationship (1) [15].

$$1 - E(n)/E_o = \beta \log [1/(1 - n/N_f)] \quad (1)$$

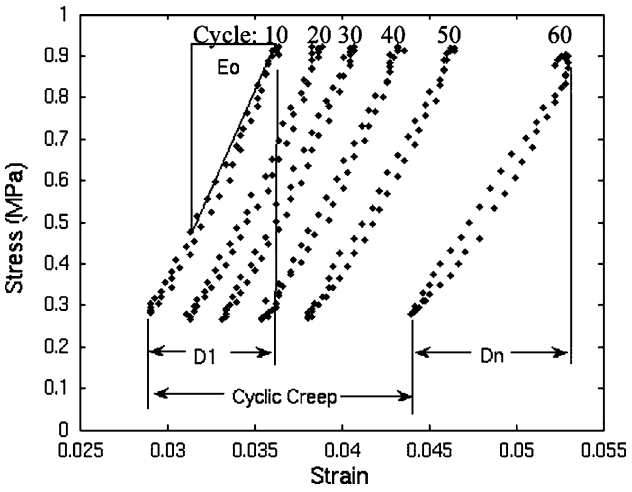

Fig. 2 Hysteresis cycles showing the components of strain accumulation; cyclic creep and damage strain = Dn–D1

where β is a dimensionless curve-fit parameter. The curve-fit parameter, β is positively correlated with effective strain, such that at higher effective strains, there is an increased rate of modulus reduction [15]. Mechanical property degradation resulting from fatigue damage accumulation in cortical bone may also describe apparent modulus degradation in trabecular bone and therefore is used to describe the same behaviour in synthetic vertebrae for this study.

Statistical analysis

A paired-observations *t*-test (POTT) was used to compare the apparent modulus of foam vs. foam with endplates in the two different strain ranges. A *t*-test (TT) was used to compare yield and ultimate properties of foam vs. foam with endplates. An analysis of covariance (ANCOVA) was used to compare linear regressions of $\Delta\sigma/E_o$ versus log (cycles to failure, N_f) between dissimilar porosity synthetic vertebrae, as well as to compare normalized cyclic creep (ε_{creep}) and normalized damage strain (ε_{damage}) versus log (cycles to failure, N_f) the two different density cellular foam constructs. A *t*-test was used to find significant differences in initial modulus between sample groups. In addition, a linear regression was performed on modulus reduction data to show the relationship between the curve-fit parameter, β for each specimen and $\Delta\sigma/E_o$.

Results

Morphology

The foam specimens consisted of an interconnected network of rods similar in morphology to human vertebral trabecular bone (Fig. 3). Results of the 3D morphological

analysis are summarized in Table 1. The material density, $\rho_{material}$ of the foam was 1.13 g/cm^3, which is approximately 40% lower than typical for human vertebral bone (1.9 g/cm^3) [17, 18].

The lower density foam has concomitant lower BV/TV, Tb.N, Tb.Th and therefore higher Tb.Sp. In comparison to human data presented in Table 1, BS/BV is within range between two different evaluations of vertebral trabecular bone and Tb.N is slightly lower. Although Tb.Th and Tb.Sp are higher, the ratio of Tb.Th/Tb.Sp is maintained between open-cell foam and vertebral bone. The higher MIL for each axis reflects the relatively larger spacing between trabeculae and thickness of trabeculae. The connectivity index, TCI is also within range for vertebral trabecular bone. The structure characterization of the foam was transverse isotropic. The open-cell foam therefore shows similar morphology to human vertebral cancellous bone, which is also transverse isotropic. Moreover, human trabecular bone has an apparent density ranging from 0.05–0.30 g/cm^3 which corresponds to a volume fraction ranging from 0.03–0.156 (assuming a bone tissue density of 1.9 g/cm^3) [7]. The foam with endplate specimens exhibited a crush or fracture consolidation typical of open-celled materials and trabecular bone where the fracture is localized to the consolidation band (Fig. 1) [17].

Static mechanical properties

Addition of the endplate increased the low strain (<0.5%) modulus of open-cell foam by 112%, whereas the high strain (0.5–1.0%) modulus was unaffected. In addition, endplates reduce non-linear behaviour in low strain by eliminating a difference between low and high strain modulus for a specimen of open-cell foam (Table 2).

The addition of endplates increased the yield strength, ultimate strength and hysteresis of open-cell foam, whereas the yield strain, ultimate strain and modulus of resilience remained unaffected (Table 3). The ultimate apparent strength and modulus of similar apparent density human vertebral cancellous bone is 0.745 MPa and 12.36 MPa, respectively [7].

Fatigue properties

Localized fracture consolidation typical of trabecular fracture, which was observed in monotonic failure of foam core samples, was also observed in fatigue failure of the synthetic vertebrae (Fig. 4). The enclosing cortex adds a component of multi-axial stress shown by the fracture in Fig. 4 of the cells closest to the vertical walls.

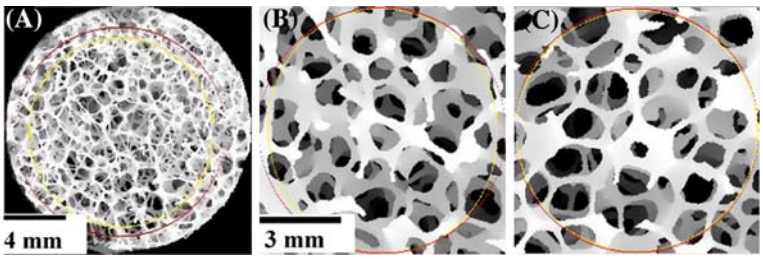

Fig. 3 μCT 3D rendering of human vertebral trabecular bone 0.089 BV/TV (**A**) and open-cell foam, 0.106 BV/TV (**B**) 0.079 BV/TV (**C**). (A) is taken from an in house report by Steffen and Keller

Table 1 Standard morphological parameters of open-cell foam and human vertebral bone

Morphology Parameter	Open-cell foam 0.09 g/cm^3	Open-cell foam 0.12 g/cm^3	Vertebral bone Steffen and Keller (n = 8, L1–L5)	Vertebral bone Cvijanovic et al. 2004 [16] (n = 48, L3)
BV/TV	0.079	0.106	0.07–0.13	0.09–0.18
BS/TV (mm^{-1})	6.263	5.298	10.51–13.24	2.1–3.4
Tb.N (mm^{-1})	0.249	0.280	0.48–0.74	1.0–1.7
Tb.Th (mm)	0.319	0.378	0.15–0.19	0.08–0.13
Tb.Sp (mm)	3.70	3.20	1.16–1.91	0.45–0.90
MIL1 (mm)	0.787	0.924	0.38–0.50	–
MIL2 (mm)	0.773	0.856	0.36–0.45	–
MIL3 (mm)	0.705	0.808	0.30–0.41	–
TCI (mm^{-1})	0.258	0.157	0.08–0.26	–

BV/TV = Volume fraction, BS/TV = Surface to volume ratio, Tb.N = Trabecular number, Tb.Th = Trabecular thickness, Tb.Sp = Trabecular spacing, MIL1,2,3 = Mean intercept length, TCI = Connectivity index

Table 2 Apparent modulus (mean ± standard deviation) of foam vs. foam with endplates separated into low and high strain ranges. Paired test with same specimen tested twice, sample size, $n = 10$

	Strain range %	Open cell foam	Foam + Endplates
Apparent Modulus E_a (MPa)	<0.5	3.04 ± 1.24*·**	6.46 ± 3.00*
	0.5–1.0	4.25 ± 2.34 **	5.60 ± 2.03

*·** Significant difference (POTT, $p < 0.05$)

Table 3 Static mechanical properties of open-cell foam with and without endplates

	Open cell foam $n = 10$	Foam + Endplates $n = 10$
Yield Strength, σ_y MPa	0.182 ± 0.013*	0.231 ± 0.033*
Yield strain, ε_y %	4.29 ± 1.06	3.44 ± 0.72
Ultimate Strength, σ_{ult} MPa	0.191 ± 0.016*	0.241 ± 0.029*
Ultimate Strain, ε_{ult} %	4.86 ± 1.17	3.78 ± 0.74
Hysteresis, H	0.220 ± 0.069*	0.461 ± 0.337*
Modulus of Resilience, E_{res} N/m^2	474 ± 120	488 ± 145

* Significant difference (t-test, $p < 0.05$)

The initial apparent modulus of synthetic vertebrae was 76 ± 17 MPa for 0.079 BV/TV based synthetic vertebrae and 78 ± 8 MPa for 0.106 BV/TV, there was no difference between the two porosity open-cell foams. During cyclic loading the modulus experienced a period of slight increase followed by non-linear degradation as strain accumulated (Fig. 5).

Equation (1) as presented by Pattin et al. was applied to each specimen, and statistically significant least squares regressions (mean $R^2 = 0.86$, standard deviation = 0.09) were obtained for modulus reduction as a function of life fraction. For all fatigue specimens β ranged from 0.118 to 0.202 (mean = 0.158, standard deviation = 0.020). A weak positive linear correlation between β and $\Delta\sigma/E_o$ was determined (Eq. 2, $R^2 = 0.12$, $p < 0.05$):

$$\beta = 3.70(\Delta\sigma/E_o) + 0.135 \quad (2)$$

The applied peak stress in the fatigue tests varied from 0.5 to 1.2 MPa. A significant non-linear correlation (least squares regression, $R^2 > 0.68$, $p < 0.05$) was obtained for

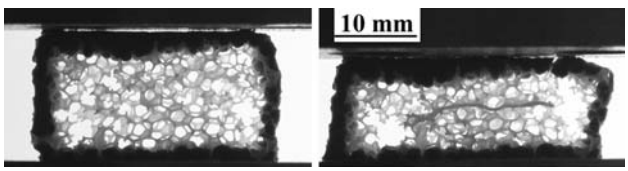

Fig. 4 After fatigue, a specimen was sectioned (left), compressed and highlighted to expose the localized fracture band (right)

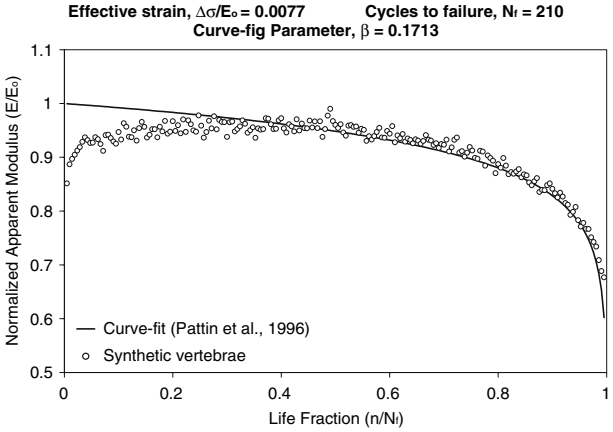

Fig. 5 Modulus reduction versus life fraction with the results of curve fitting equation (1)

$\Delta\sigma/E_o$ versus log (N_f) for fatigue failure less than 10^4 cycles (Fig. 6). There was no difference in the fatigue behaviour presented between dissimilar volume fraction synthetic vertebrae. Greater than 10^4 cycles (<0.004 effective strain), samples appear to approach the fatigue failure endurance limit.

Fatigue strain accumulation was broken into two components, cyclic creep and damage strain as described previously in the methods. Cyclic creep was a dominant contributor for total strain accumulation during cyclic loading. Significant positive linear relationships were obtained for cyclic creep vs log cycles (least squares regression, $R^2 > 0.33$, $p < 0.05$) (Fig. 7). There was no difference between the mean strain at failure for 0.106 BV/TV and 0.079 BV/TV synthetic vertebrae, 4.80 ± 1.58% and 5.68 ± 1.33% respectively.

Discussion

Variability in physical and mechanical properties of human and animal vertebral bone present a challenge to

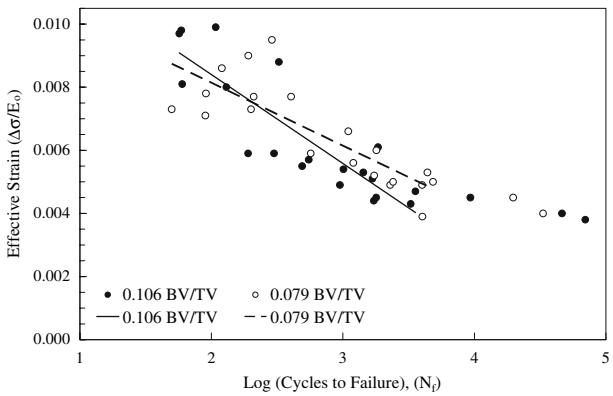

Fig. 6 S-N Curves for two different porosity open-cell foam based synthetic vertebrae

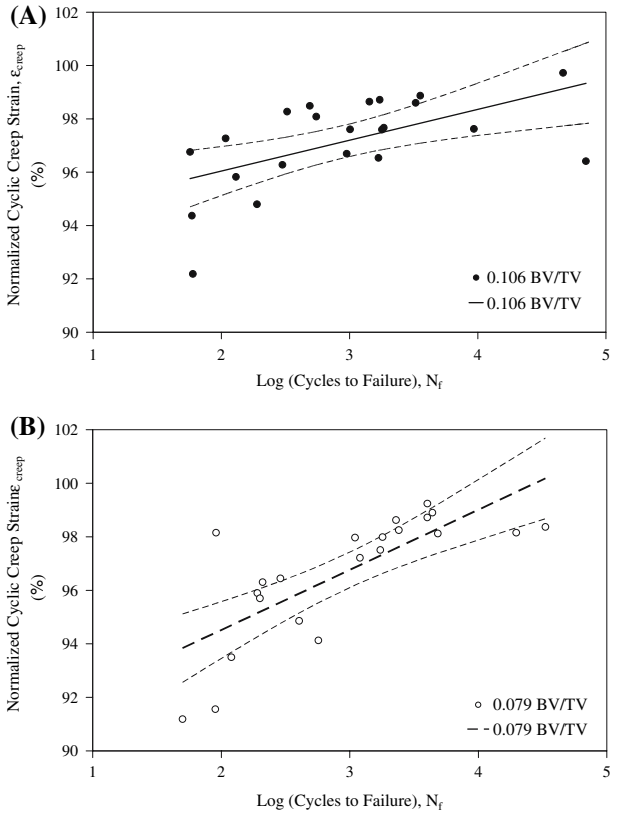

Fig. 7 Proportion of cyclic creep strain versus log (cycles to failure) for dissimilar porosity open-cell foam based synthetic vertebrae. The dashed lines indicate 95% confidence intervals. (**A**) 0.106 BV/TV (**B**) 0.079 BV/TV

researchers who are studying emerging surgical treatments for osteoporotic vertebral fractures and tumors such as vertebroplasty and kyphoplasty. Osteoporosis is a degenerative disease that reduces bone strength and bone mass particularly in trabecular bone, where bone mass reductions occur up to ten times greater than compact bone [19]. Osteoporotic vertebral compression fracture and cement augmentation studies typically rely on cadaver vertebrae [20–22], which exhibit highly variable structural and material characteristics depending on the age and degeneration of the samples. To address this issue, a synthetic thoracic vertebral model was created with a geometrically simplified cylindrical foam core and an enclosing fiberglass resin cortex. Morphology, static and dynamic (fatigue) mechanical properties of the synthetic vertebrae were evaluated and compared to natural trabecular bone.

The ultimate compressive stress of the open-cell foam obtained in this study agrees with the value reported by the manufacturer, but the compressive modulus was substantially lower. The manufacturer lists the σ_{ult} and E_a for the open-cell foam as 0.24 MPa and 18.6 MPa, respectively. The three-fold higher modulus may be explained by larger test specimens used by the manufacturer, (63.5 mm by 63.5 mm by 19 mm), which is considerably larger than the foam cores in this study. The size of a cellular material being tested has an influence on the modulus, where the measured modulus is lower for small samples (10 mm height and 81 mm^2 cross-sectional area), and this effect is amplified by higher porosities [23].

The open-cell rigid foam examined in this study exhibited 3D morphology similar to human vertebral cancellous bone, which is transversely isotropic and comprised of an integrated network of thin, interconnected bone trabeculae. The foam showed similar connectivity, but was comprised of thicker and more widely spaced elements in comparison to trabeculae in human cancellous bone. Consequently, the apparent modulus and strength of the foam cores (with and without endplates) was lower than reported for similar porosity human cancellous bone, which also reflects the lower material density of the foam in comparison to natural bone. Yield and ultimate strain were also substantially lower than human vertebral trabecular bone, which are reported as 6.0% and 7.4%, respectively [18].

Although the synthetic vertebrae were comprised of a lower material density cancellous core and cortical cortex than human trabecular bone, and did not contain bone marrow, the mechanical behaviour (apparent stiffness) of the synthetic vertebrae was similar to cadaveric thoracic vertebrae [24]. Comparison of S-N curves to bovine and human trabecular bone in literature shows that open-cell foam based synthetic vertebrae had similar fatigue results (Fig. 8). The samples of trabecular bone tested in literature were cored samples [4, 9, 14, 25]. Unlike the synthetic vertebrae tested in this study, cored samples of trabecular bone do not have an enclosing cortex. The inclusion of a lateral cortical shell alters the stress distribution from one of uniaxial to multiaxial compression. This difference in

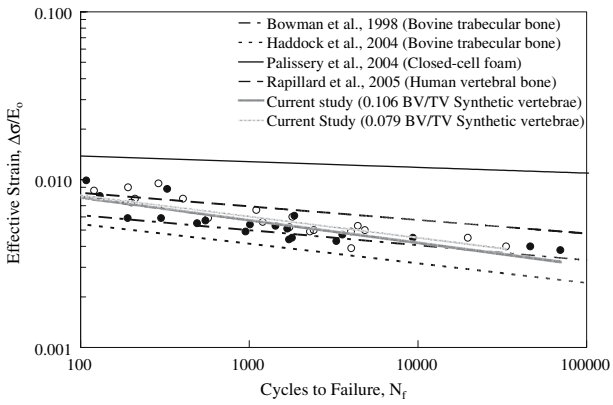

Fig. 8 Comparison of S-N curves of open-cell foam based synthetic vertebrae with human vertebral trabecular bone [25], bovine trabecular bone [9], [14] and closed-cell foam [4]

boundary conditions may have produced the steeper slope of the S-N curve for the synthetic vertebrae.

Modulus degradation of synthetic vertebrae was comparable to reported fatigue of cortical bone as shown by the fitted relationship between normalized modulus and life fraction. The curve-fit parameter reported for cortical bone ranged from 0.03 to 0.96 for an effective strain range of 0.004 to 0.009 respectively [15], whereas for synthetic vertebrae the range of the curve-fit parameter was narrower from 0.12 to 0.20. A narrow range for the curve-fit parameter indicates that the rate of modulus reduction in synthetic vertebrae changes less with effective strain in comparison to cortical bone. Furthermore, the relationship determined between modulus reduction and effective strain by using Eqs. (1) and (2) may be used to predict the fatigue behaviour of the synthetic vertebrae.

In summary, the morphology and mechanical behaviour of the foam-core, synthetic thoracic vertebral centrum is consistent with human vertebral trabecular bone and vertebral bodies, indicating that open-cell foam synthetic vertebrae appear to be a promising alternative for both static or fatigue studies of human vertebrae. Synthetic vertebrae with an open-cell core would be useful in cement augmentation research for studying the effects of cement volume, composition and placement strategy on fatigue behaviour. In addition, various porosity foams could simulate different degrees of osteoporosis degeneration, allowing for fatigue testing of prophylactic repair. Synthetic vertebrae may also be used to assess the performance of orthopaedic devices.

Acknowledgements Research supported by the Vermont Space Grant Consortium and NASA EPSCoR. Special thanks to Thomas Steffen for human vertebral μ-CT images, and Jeremy Lemoine and Michael Liebschner for μ-CT scanning of the open-cell foam.

References

1. C. J. HERNANDEZ, G. S. BEAUPRE, T. S. KELLER and D. R. CARTER, *Bone.* **29** (2001) 74
2. J. A. SZIVEK, M. THOMAS and J. B. BENJAMIN, *J. Appl. Biomater.* **4** (1993) 269
3. A. D. HEINER and T. D. BROWN, *J. Biomech.* **34** (2001) 773
4. V. PALISSERY, M. TAYLOR and M. BROWNE, *J. Mater. Sci. Mater. Med.* **15** (2004) 61
5. A. HARTE, N. FLECK and M. ASHBY, *Acta. Mater.* **47** (1999) 2511
6. L. GIBSON, *J. Biomech.* **38** (2005) 377
7. T. S. KELLER, *J. Biomech.* **27** (1994) 1159
8. A. PARFITT, C. MATHEWS, A. VILLANUEVA, M. KLEEREKOPER, B. FRAME and D. RAO, *J. Clin. Invest.* **72** (1983) 1396
9. S. BOWMAN, X. GUO, D. CHENG, T. KEAVENY, L. GIBSON, W. HAYES and T. MCMAHON, *J. Biomech. Eng.* **120** (1998) 647
10. T. S. KELLER and M. NATHAN, *J. Spinal Disord.* **12** (1999) 313
11. M. PANJABI, K. TAKATA, V. GOEL, D. FEDERICO, T. OXLAND, J. DURANCEAU, and M. KRAG, *Spine* 16 (1991) 888
12. H. WILKE, P. NEEF, M. CAIMI, T. HOOGLAND and L. CLAES, *Spine* **24** (1999) 755
13. D. LINDSEY, M. KIM, M. HANNIBAL and T. ALAMIN, *Spine* **30** (2005) 645
14. S. HADDOCK, Y. OSCAR, M. PRAVEEN, W. ROSENBERG and T. KEAVENY, *J. Biomech.* **37** (2004) 181
15. C. A. PATTIN, W. E. CALER and D. R. CARTER, *J Biomech* **29** (1996) 69
16. O. CVIJANOVIC, D. BOBINAC, S. ZORICIC, Z. OSTOJIC, I. MARIC, Z. CRNCEVIC-ORLIC, I. KRISTOFIC and L. OSTOJIC, *Spine* **29** (2004) 2370
17. A. NAZARIAN and R. MULLER, *J. Biomech.* **37** (2004) 55
18. T. H. HANSSON, T. S. KELLER and M. PANJABI, *Spine* **11** (1986) 56
19. V. KOSMOPOULOS and T. S. KELLER, *Eur. Spine J.* **13** (2004) 617
20. S. M. BELKOFF, J. M. MATHIS, L. E. JASPER and H. DERAMOND, *Spine* **26** (2001) 1537
21. S. TOMITA, S. MOLLOY, L. E. JASPER, M. ABE and S. M. BELKOFF, *Spine* **29** (2004) 1203
22. R. K. WILCOX, *Proc. Inst. Mech. Eng. [H]* **218** (2004) 1
23. M. ZHU, T. KELLER and D. SPENGLER, *J. Biomech.* **27** (1994) 57
24. D. MCCUBBERY, D. CODY, E. PETERSON, J. KUHN, M. FLYNN and S. GOLDSTEIN, *J. Biomech.* **28** (1995) 891
25. L. RAPILLARD, M. CHARLEBOIS and P. ZYSSET, *J. Biomech.* **39** (2006) 2133